Sustainable High Yield Production of Cellulose Nanomaterials for Easy-cleaning Surfaces of Cellulose-based Materials

Wangxia Wang,[a,b] Nanxun Sun,[b] Zhaosheng Cai,[b] Kaijin Sun,[a] Feng Gu,[b,c,*] Yongcan Jin,[d,*] and Huining Xiao [e]

Cellulose nanomaterials with high yield and desired properties were sustainably produced using a facile recyclable acid treatment (oxalic acid) with mineral acid catalysis at ambient pressure. The resultant nanocellulose was uniform in dimensions (diameter and length distributions) and highly dispersible in the aqueous phase. The nanocellulose with yield up to 33.9%, a zeta potential of -53.9 mV, and 100% volume stability (24 h) was achieved *via* oxalic acid treatment in conjunction with sulfuric acid addition. The coating of such nanocellulose on paper created a uniform and dense layer on the surface, which lowered Gurley air permeability (*i.e.*, prolonging the time required for air flow from 3.9 to 681.9 s per 100 mL). Moreover, the coated paper showed a complete grease barrier after 48 h and presented easy-cleaning behavior. The approach developed in this work offers an adoptable guidance to design green and sustainable easy-cleaning surfaces. In turn, this approach will provide potential applications of nanocellulose for green based packaging and environmental protection.

Keywords: Nanocellulose; Yield; Dispersible; Grease barrier; Easy-cleaning

Contact information: a: Jiangsu R&D Center of the Ecological Textile Engineering & Technology, Yancheng Polytechnic College, Yancheng, 224005, China; b: School of Chemistry and Chemical Engineering, Yancheng Institute of Technology, Yancheng, 224001, China; c: Jiangsu Provincial Key Lab of Biomass Energy and Materials, Nanjing, 210042, China; d: Jiangsu Provincial Key Lab of Pulp and Paper Science and Technology, Nanjing Forestry University, Nanjing 210037, China; e: Department of Chemical Engineering, University of New Brunswick, Fredericton, NB, E3B 5A3, Canada;
** Corresponding authors: gufeng8411@outlook.com; jinyongcan@njfu.edu.cn*

INTRODUCTION

Functional surfaces mimicking naturally occurring systems, such as lotus leaves, and rendering the materials low surface energies for preventing adhesion of stains are of great importance for various applications. Self-cleaning or easy-cleaning surfaces can be developed by application of carbon or silica-based nanocomposite coatings based on the surface micro/nano-morphologies, while one of the significant drawbacks of these artificial surfaces is that they are weak and easily abraded (Wu *et al*. 2013; Lu *et al*. 2015). However, the recycling issue and biocompatibility of inorganic composite coated cellulose-based materials offer challenges. Nanocellulose has attracted much attention due to its nano size, light weight, high surface area, and excellent mechanical and barrier properties. Furthermore, it is biocompatible, recyclable, and biodegradable. Nanocellulose has great potential to be used as a reinforcement for bio-composites and barrier-absorbent materials in environmental protection. Its application can be readily extended to paper packaging and biomedical areas (Moon *et al*. 2016; Gu *et al*. 2018, 2019; Mithilesh and Fang 2019; Dai *et al*. 2019).

Many efforts have been devoted to the effective production of nanocellulose. Physical mechanical fibrillation, chemical acid hydrolysis, and biological/enzymatic degradation are the main approaches applied (Saito *et al*. 2005; Abdul Khalil *et al*. 2014; Wang *et al*. 2016; Kontturi *et al*. 2018; Narkpiban *et al*. 2019). Concentrated mineral acid hydrolysis as a quick and energy-saving method has been widely used for cellulose nanocrystals (CNC) production, such as sulfuric acid and hydrochloric acid hydrolysis (Camarero *et al*. 2013; Liu *et al*. 2014; Wang *et al*. 2014; Du *et al*. 2017). However, difficulties in economical acid recovery and the strict equipment requirement are still the main concerns for concentrated mineral acid utilization. Oxalic acid can be easily recovered by recrystallization at room temperature, which means that it could be applied as a green reagent for functional nanocellulose production. However, the relatively high p*K*a value (1.25) of oxalic acid resulted in a mild acid condition, which showed limited cellulose hydrolysis. The CNC yield by oxalic acid hydrolysis was less than 20% and the resultant CNC exhibited poor dispersion stability even with an acid concentration of 60 wt% at 120 °C (Chen *et al*. 2016; Bian *et al*. 2017; Wang *et al*. 2017).

Stable dispersion is a prerequisite for functional applications of nanocellulose with ideal properties (Isogai 2013; Jorfi and Foster 2015; Jung *et al*. 2015; Tyagi *et al*. 2019). Nanocellulose dispersion for a paper coating mixture could benefit the formation of uniform and dense networks on the paper surface, thus blocking the grease molecular penetration pathway and lowering air permeability. In this work, sulfuric acid (p*K*a = -3.0) and hydrochloric acid (p*K*a = -8.0) with low p*K*a values were used to boost the oxalic acid hydrolysis of cellulose. Effects of mineral acid (H_2SO_4/HCl) on the yield of oxalic acid hydrolyzed nanocellulose, dispersion stabilities, and other properties were systematically investigated. Influences of nanocellulose on dispersant stability on grease barriers and easy-cleaning behaviors of cellulose-based materials were also characterized.

EXPERIMENTAL

Materials

Bleached kraft eucalyptus pulp (BEP) was used as the feedstock for nanocellulose production, which was kindly provided by a pulp mill in Shandong, China. Glucan, xylan, and lignin contents of BEP were 77.6%, 16.1%, and 0.9%, respectively. Sulfuric, hydrochloric, and oxalic acids were purchased from Sigma-Aldrich (St Louis, MO), and used without further purification. Fisher brand P4 grade filter paper (Fisher Scientific, Pittsburgh, PA) was used as a base paper for nanocellulose coating.

Cellulose Nanocrystals (CNC) Production

The procedure of CNC production is shown in Fig. 1. Concentrated acid solution was prepared by dissolving a certain amount of solid oxalic acid (40 wt%) in water at 90 °C with magnetic stirring. Sulfuric or hydrochloric acid of 10 wt% was added to the oxalic acid solution. BEP was then subjected to the concentrated acid solution with a fiber content of 5% (weight per volume) for 4 h with continuous stirring at 90 °C. The acid hydrolysis was terminated by adding 100 mL of deionized water and was then vacuum filtrated to separate the fiber and soluble components. The separated fiber was dialyzed with a 7000-cut-off regenerated cellulose membrane to remove residual acid. Centrifuged (2603 g, 5 min) CNC was received and stored at 4 °C for characterization and surface coating. For comparison, sulfuric acid hydrolyzed CNC was prepared at an

optimized condition with an acid concentration of 58 wt%, hydrolysis temperature of 56 °C, and a time of 100 min.

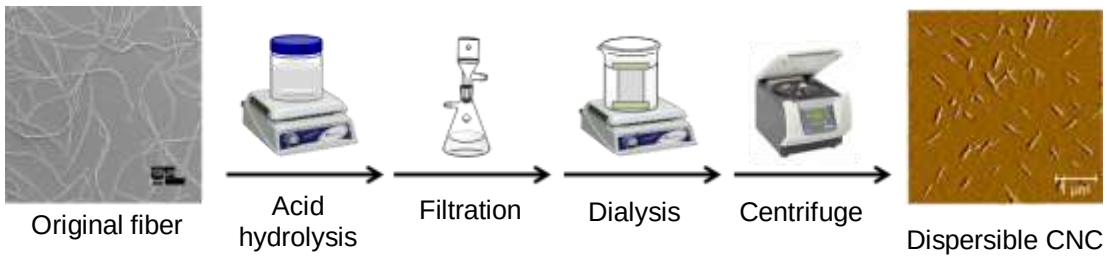

Fig. 1. Sustainable, high yield production of nanocellulose

CNC Characterization

Morphology of CNC (0.005%, weight per volume) was observed by Atomic Force Microscopy (AFM, Nanoscope IIIa, Veeco Instruments Inc., Santa Barbara, CA). The images were scanned in multimode in air using a commercial silicon-tapping probe (NP-S20, Veeco Instruments, Plainview, NY) with a spring constant of 0.32 N/m, a resonance frequency of 273 kHz, and settings of 512 pixels/line and Hz scan rate. The zeta potential of CNC (0.1%, w/v) was measured by a Zeta potential analyzer (Nanobrook Omni, Brookhaven Instruments Corp., Holtsville, NY, USA). Carboxyl group content of CNC was determined by conductometric titration using an automatic titrator (AUT-701, TOADKK, Japan) (Guo *et al*. 2019). The dispersion stability of CNC suspension was characterized by measuring the volume stability of the fiber layer. The fiber suspension with a fixed volume (20 mL) and concentration (0.5%, w/v) was first magnetically stirred for 30 min, and then transferred to 25 mL of burette. Those steps were followed by measuring the fiber layer volume at 1 min and 24 h. The volume stability was calculated with Eq. 1,

$$V\,(\%) = (V_t \div V_0) \times 100 \quad (1)$$

where V_0 is the fiber layer volume at 1 min, and V_t is the fiber layer volume at 24 h.

Fourier transform infrared spectroscopy (FTIR, Nicolet 6700, Thermo Scientific, QC, Canada) spectra were collected between 4000 and 400 cm^{-1} wavenumbers. The X-ray diffraction (XRD) analysis was performed on a Bruker D8 Advance spectrometer (Karlsruhe, Germany). Samples for XRD were scanned in the range of 5 to 50 ° (2θ). A step size of 0.02 ° and a step time of 1.0 s were used during the measurements. The crystallinity of acid hydrolyzed CNC was calculated according to the Segal peak height method (Segal *et al*. 1959) with Eq. 2,

$$CrI\,(\%) = [(I_{200} - I_{am}) \div I_{200}] \times 100 \quad (2)$$

where I_{200} is the diffraction intensity associated with crystalline cellulose (maximum diffraction between the scattering angles of 2θ = 22 ° and 23 °), and I_{am} is the intensity associated with amorphous cellulose (minimum diffraction between the scattering angles of 2θ = 18 ° and 19 °) (Ítalo *et al*. 2017).

CNC Coating and Paper Properties

CNC (1.0%, weight per volume) was directly coated onto the surface of a filter paper with a bar-coating machine (K303 Multi-coater, RK Print Coat Instruments Ltd,

United Kingdom). A Mayer rod No. 4 was used at a coating speed of 2.0 m/min. Afterward, the coated paper samples were dried at ambient temperature to remove 80 to 90% moisture followed by oven drying at 60 °C overnight under pressure to minimize deformation. Oven-dried coated papers were weighed for calculating coating weights.

The barrier property against vegetable oil of CNC coated papers was characterized according to the TAPPI standard method T507 cm-99 (1999) by calculation of the grease stained area of the stain absorber. For more accurate results, a scanner (CanoScan, LiDE 700F) was employed to check the grease-stained area in this study. Assemblies prepared with a bed plate, a foil separator, clean blotter paper (stain absorber), the test specimen, and saturated blotter paper (Sudan III dyed vegetable oil) covered with the pressure block (400 g) from bottom to top, were placed in the oven for 48 h at 60 °C. The grease stained blotter paper was scanned every 4 h when necessary. Finally, the percentage of the grease stained area was calculated by Photoshop software and reported as the average of two measurements with standard deviations.

The surface morphology of CNC coated paper was observed by a Scanning Electron Microscope (SEM, JSM-6400, JEOL, Tokyo, Japan). Tensile properties were measured based on the TAPPI T494 om-13 (2013) method by using an L&W tensile tester (Lorentzen and Wettre, Kista, Sweden) equipped with a 500 N load cell at a crosshead speed of 12 mm/min. Porosity was measured according to the TAPPI T460 om-11 (2011) using a Gurley air permeability tester 4110 (Teledyne Gurley, Troy, NY, USA). Easy-cleaning behavior of the CNC coated paper was characterized as follows: a 3 by 3 cm square control filter paper (FP) and a CNC coated filter paper (CNC-FP) was prepared while gently releasing one drop of Sudan III dyed oil on the paper surface for 15 seconds, and then the surface was wiped with a clean tissue. Pictures were captured and recorded during the process.

RESULTS AND DISCUSSION

Nanocellulose Fractionation

The yield and surface charge of centrifuged cellulose fractions from acid hydrolysis are shown in Table 1. During oxalic acid hydrolysis, cellulose carboxylation by dicarboxylic acid through the esterification of one carboxyl group occurred (Chen *et al*. 2016). The yield of oxalic acid-hydrolyzed CNC (CNC-O40) was only 9.2% with a zeta potential of -45.4 mV. A large amount of residue (80.8%) indicated that hydrolysis was limited under the weak acid condition. Increasing oxalic acid concentration from 40% to 60% and increasing the hydrolysis temperature from 90 °C to 110 °C slightly improved CNC yield. However, the result was still less than 20% either with 50% at 100 °C or 60% at 110 °C (data not listed).

After mineral acid catalysis, CNC yield and zeta potential (absolute value) can be improved effectively. A yield up to 33.9% with a zeta potential of -53.9 mV was achieved by sulfuric acid catalysis (CNC-O40S10), which was 25.2% and -51.6 mV for hydrochloric acid catalysis (CNC-O40C10). CNC from concentrated sulfuric acid hydrolysis (CNC-S58) was also prepared for comparison. Results indicated the yield and zeta potential of CNC-O40S10 were comparable to those of CNC-S58 (Jiang and Hsieh 2013; Sun *et al*. 2017). Besides, oxalic acid hydrolysis produced a large portion (45.6% to 80.8%) of partial carboxyl-functionalized hydrolysis residue (precipitant). The hydrolysis residue has a higher surface charge and shorter fiber length than the original

fiber, which could be used as a resource for further application or re-hydrolysis. The hydrolysis residue from traditional concentrated sulfuric acid treatment was only 12.8% at an acid concentration of 58 wt% and a reaction time of 100 min at 56 °C.

Table 1. Characterization of Centrifuged Cellulose Fractions

Samples	Supernatant (CNC)		Precipitate (Hydrolysis residue)	
	Yield, %	Zeta potential, mV	Yield, %	Zeta potential, mV
CNC-O40 [a]	9.2 (0.2)	-45.4 (0.6)	80.8 (0.5)	-32.5 (0.2)
CNC-O40C10 [b]	25.2 (0.3)	-51.6 (0.5)	56.5 (0.6)	-32.7 (0.4)
CNC-O40S10 [c]	33.9 (0.3)	-53.9 (0.3)	45.6 (0.7)	-33.1 (0.3)
CNC-S58 [d]	35.2 (0.4)	-54.2 (0.5)	12.8 (0.5)	-35.1 (0.5)

[a] Oxalic acid (40 wt%); [b] Oxalic acid (40 wt%) with 10 wt% HCl; [c] Oxalic acid (40 wt%) with 10 wt% H_2SO_4; [d] Sulfuric acid (58 wt%). Standard deviations are given in parentheses.

CNC Characterization

CNC morphologies characterized by AFM are shown in Fig. 2. Three CNC samples (CNC-O40, CNC-O40C10, and CNC-O40S10) were prepared under the same consistency and procedure for AFM analysis. A higher surface charge and smaller particle size can help form a more stable dispersed suspension (Niu *et al*. 2017). Due to the relatively low surface charge (-45.4 mV), fiber aggregates can be clearly found from Fig. 2a (CNC-O40). Mineral acid catalysis can produce CNC with a stronger surface charge, which resulted in a higher dispersion stability according to the AFM images (Fig. 2b & c). Sulfuric acid catalyzed CNC (CNC-O40S10) exhibits a desirable size uniformity with an average length at 418 nm and a diameter of 39 nm as calculated by Image J software (National Institute of Health, MD, USA). The product is comparable to CNC prepared by concentrated sulfuric acid hydrolysis (Wang *et al*. 2012).

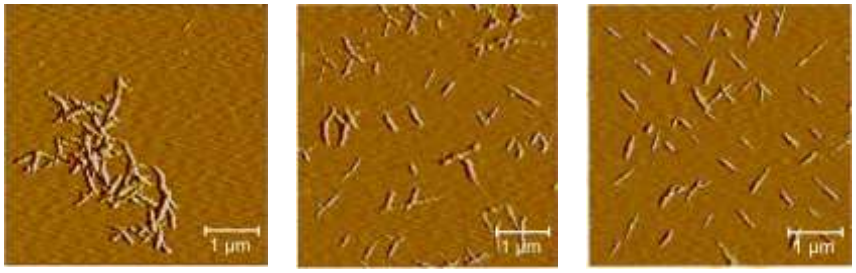

(a) CNC-O40 **(b)** CNC-O40C10 **(c)** CNC-O40S10

Fig. 2. The morphologies of nanocellulose characterized by AFM (Scale: 1 µm)

The dispersion stability of CNC suspension is also characterized according to the volume stability of the fiber layer. The volume stabilities were 80.8%, 96.8%, and 100% for CNC-O40, CNC-O40C10, and CNC-O40S10, respectively (Fig. 3). Mineral acid with low p*K*a can boost esterification and increase the carboxyl group content of cellulose. The characteristic peak of the carbonyl group (FTIR, C=O, 1730 cm^{-1}) was observed for CNC-O40, CNC-O40C10, and CNC-O40S10 (Fig. 4); whereas the C=O signals of mineral acid catalyzed CNC were much stronger than those hydrolyzed by oxalic acid. This suggests the higher degree of esterification. Carboxyl group contents determined by conductometric titration were 0.11, 0.32, and 0.42 mmole/g-CNC, respectively for CNC-O40, CNC-O40C10, and CNC-O40S10. Increasing surface charge by introducing

carboxyl groups *via* mineral acid catalysis was found to be helpful for producing stable dispersed nanocellulose.

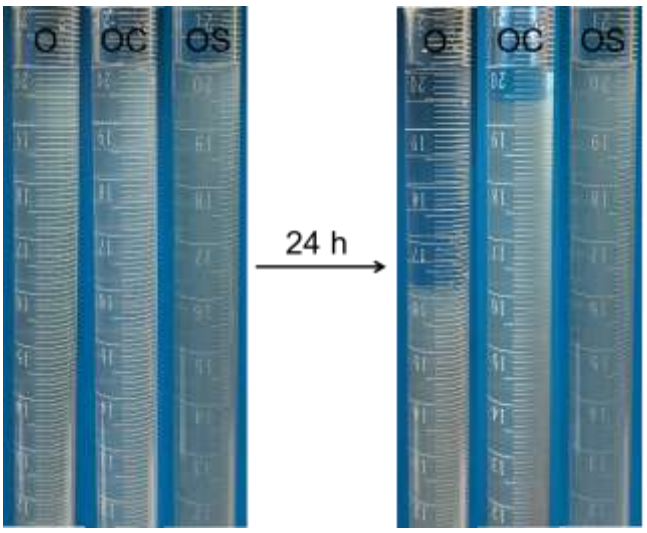

Fig. 3. Dispersion stability of CNC suspension (O: CNC-O40; OC: CNC-O40C10; OS: CNC-O40S10).

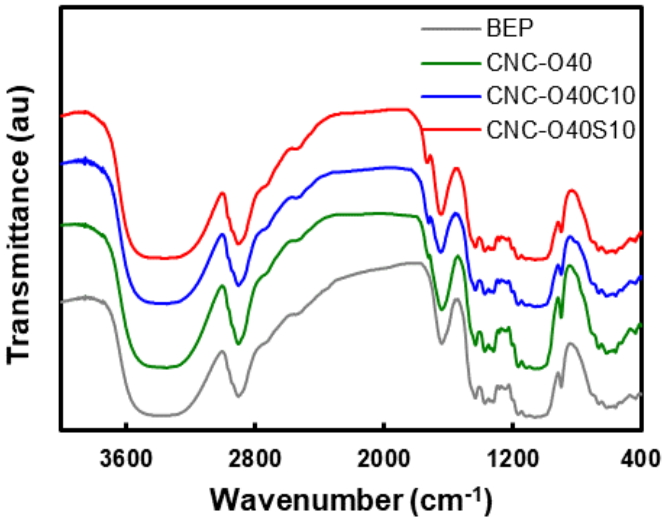

Fig. 4. FTIR spectra of nanocellulose

XRD patterns of original BEP and CNC exhibited a typical cellulose I crystalline structure (JCPDS 03-0289), with XRD peaks located at 14.9 °, 16.2 °, 22.7 °, and 34.5 ° corresponding to ($1\bar{1}0$), (110), (200), and (004) reflection planes, respectively (Sun *et al*. 2015).

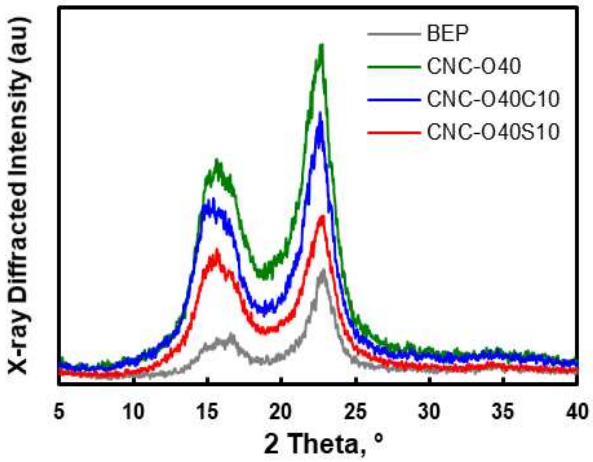

Fig. 5. X-ray diffraction (XRD) patterns of nanocellulose

According to the XRD curves (Fig. 5), the crystallinity of the original bleached eucalyptus pulp was 78.0%, which was decreased to 66.3%, 71.8%, and 68.0% with 40% oxalic acid hydrolysis, HCl, and H_2SO_4 catalysis, respectively. The amorphous part of cellulose undergoes preferential acidic hydrolysis when compared to crystalline domains (Kargarzadeh *et al*. 2012). Mild oxalic acid CNC showed a lower crystallinity than the original fiber. This might be caused by the insoluble oligomers being degraded by mild acid, then reabsorbed onto the fiber surface, and decreased crystallinity (Xu *et al*. 2017). The lowered crystallinity of cellulose after oxalic acid hydrolysis provides the potential for monosaccharide production with increased accessibility.

Paper Properties with CNC Coating

The grease barrier property of CNC coated paper was determined by the grease stained area under standard pressure and temperature according to the T507 cm-99 method. The CNC coating weights were all adjusted to 6 g/m^2. Grease stained areas (%) of coated filter paper are shown in Table 2. The grease-stained area of uncoated filter paper was 16.6% at 4 h, which was further increased to 77.0% with the incubation time extended to 48 h at 60 °C. This indicates the weak grease barrier. Coating solid surfaces with cellulose nanofibrils *via* physical deposition was found to keep the surfaces free of a variety of oils, ranging from viscous engine oil to polar n-butanol upon water action (Huang and Wang 2017). The grease stained area of CNC-O40 coated paper was reduced to 24.2% at 48 h. The value can be further reduced to 2.8% for CNC-O40C10 coated paper, and the complete grease barrier was achieved by CNC-O40S10 coating.

Table 2. Grease Stained Area of CNC Coated Paper (Coating Weight: 6 g/m^2)

Coating paper	4 h, %	8 h, %	24 h, %	48 h, %
Control-FP	16.6 (0.6)	30.9 (0.9)	62.4 (0.8)	77.0 (0.9)
CNC-O40-FP	ND	ND	8.9 (0.5)	24.2 (0.7)
CNC-O40C10-FP	ND	ND	ND	2.8 (0.6)
CNC-O40S10-FP	ND	ND	ND	ND
FP: Filter paper; ND: Not detectable; Standard deviations are given in parentheses.				

The stability of CNC dispersion is closely related to its performance in application. The highly dispersed CNC after acid catalysis is beneficial for forming a uniform and dense film on the paper surface after coating. This uniform and dense film could increase hydrogen bonding between fibers and decrease paper porosity, thus leading to an effective barrier for penetrating grease molecules (Fig. 7). The hydrogen bonding formed between CNC and the cellulose of the base paper can be confirmed by the increased tensile strength of the CNC coated paper, *i.e.*, 1.9 kN/m and 3.1 kN/m for the control base paper and CNC-O40S10 coated paper, respectively. Gurley porosity measures the time taken by a determined air volume (100 mL) to pass through paper samples. Therefore, longer time means lower porosity. The measured time was 3.9 s for the control base paper, which was increased to 681.9 s for CNC-O40S10 coated paper. This indicated much lower porosity by CNC coating. As shown in the SEM images below (Fig. 7), most pores of base paper are covered with nano-sized particles, which provide effective shielding against small molecular penetration and improve paper barrier properties.

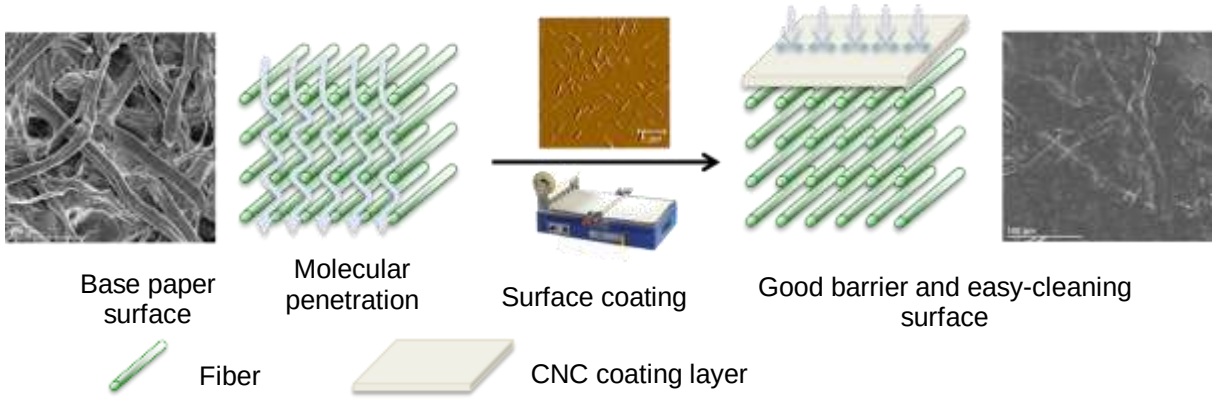

Fig. 6. Uniform and dense nanocellulose layer for improving barrier properties of cellulose-based materials

Figure 7 illustrates the easy-cleaning behavior of a cellulose based material by CNC coating. Once contaminated by Sudan III dyed oil, the control filter paper (FP) can absorb the oil very fast (Fig. 7b). After 15 s, most contaminates were absorbed (Fig. 7c) and cannot be wiped away (Fig. 7d). For CNC coated paper, Sudan III dyed oil remained unchanged on the surface with extended stain time (Fig. 7f and Fig. 7g) and can be easily cleaned up (Fig. 7h). The easy-cleaning behavior of CNC coated paper can expand the application of cellulose based materials in our daily life and provide environmental protection with renewability and recyclability.

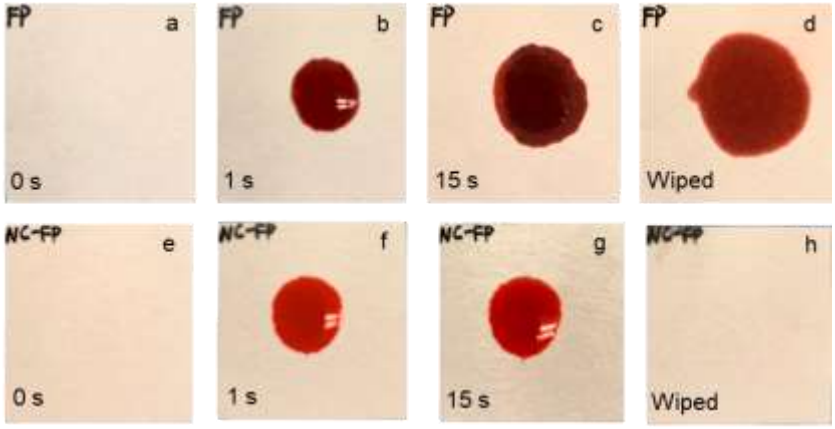

Fig. 7. Surface contaminated by Sudan III dyed oil and wiped by a clean tissue (a-d: filter paper; e-h: CNC coated paper)

CONCLUSIONS

1. Dispersible (zeta potential at -54 mV) nanocellulose was effectively prepared *via* facile process catalyzed by 40% oxalic acid treatment in conjunction with 10% H_2SO_4 addition.
2. The yield of CNC was increased to 33.9%, compared to 9.2% in the absence of sulfuric acid.
3. The highly dispersible nanocellulose facilitates the coating and enables the forming of a uniform and dense layer on the paper surface. The coated paper showed a complete grease barrier after 48 h and easy-cleaning behavior.
4. The application of as prepared CNC could be readily extended to a variety of areas related to green based packaging and provide environmental protection.

ACKNOWLEDGMENTS

The authors are grateful for the financial support from the Natural Science Foundation of Jiangsu Provincial Key Lab of biomass energy and materials, Grant No. JSBEM201810, Yancheng Polytechnic College Provincial Research Platform, Grant No. YGKF-201706, Natural Science Foundation of Jiangsu Province, Grant No. BK20181051 and BK20181052, China Postdoctoral Science Foundation, Grant No. 2018M640490, National Natural Science Foundation of China (No. 21908188), and NSERC Canada.

REFERENCES CITED

Abdul Khalil, H. P. S., Davoudpour, Y., Islam, M., Mustapha, A., Sudesh, K., Dungani, R., and Jawaid, M. (2014). "Production and modification of nanofibrillated cellulose using various mechanical processes: A review," *Carbohyd. Polym.* 99, 649-665. DOI: 10.1016/j.carbpol.2013.08.069

Bian, H., Chen, L., Dai, H., and Zhu, J. (2017). "Integrated production of lignin containing cellulose nanocrystals (LCNC) and nanofibrils (LCNF) using an easily recyclable di-carboxylic acid," *Carbohyd. Polym.* 167, 167-176. DOI: 10.1016/j.carbpol.2017.03.050

Camarero, E., Kuhnt, T., Foster, E., and Weder, C. (2013). "Isolation of thermally stable cellulose nanocrystals by phosphoric acid hydrolysis," *Biomacro.* 14, 1223-1230. DOI: 10.1021/bm400219u

Chen, L., Zhu, J., Baez, C., Kitin, P., and Elder, T. (2016). "Highly thermal-stable and functional cellulose nanocrystals and nanofibrils produced using fully recyclable organic acids," *Green Chem.* 18, 3855-3843. DOI: 10.1039/c6gc00687f

Dai, L., Cao, Q., Wang, K., Han, S., Si, C., Liu, D., and Liu, Y. (2019). "High efficient recovery of L-lactide with lignin-based filler by thermal degradation," *Ind. Crop. Prod*. 143, 111954-111962. DOI: 10.1016/j.indcrop.2019.111954

Du, H., Liu, C., Zhang, Y., Yu, G., Si, C., and Li, B. (2017). "Sustainable preparation and characterization of thermally stable and functional cellulose nanocrystals and nanofibrils *via* formic acid hydrolysis," *J. Biores. Bioprod.* 2, 10-15. DOI: 10.21967/jbb.v2i1.68

Gu, F., Wang, W., Cai, Z., Xue, F., Jin, Y., and Zhu, J. (2018). "Water retention value for characterizing fibrillation degree of cellulosic fibers at micro and nanometer scales," *Cellulose* 25, 2861-2871. DOI: 10.1007/s10570-018-1765-8

Gu, L., Jiang, B., Song, J., Jin, Y., and Xiao, H. (2019). "Effect of lignin on performance of lignocellulose nanofibrils for durable superhydrophobic surface," *Cellulose* 26, 933-944. DOI: 10.1007/s10570-018-2129-0

Guo, T., Gu, L., Zhang, Y., Chen, H., Jiang, B., Zhao, H., Jin, Y., and Xiao, H. (2019). "Bioinspired self-assembled films of carboxymethyl cellulose–dopamine/ montmorillonite," *J. Mater. Chem. A.* 7, 14033-14041. DOI: 10.1039/C9TA00998A

Huang, S., and Wang, D. (2017). "A simple nanocellulose coating for self-cleaning upon water action: molecular design of stable surface hydrophilicity," *Angew. Chem. Int. Edit.* 56, 9053-9057. DOI: 10.1002/ange.201703913

Isogai, A. (2013). "Wood nanocelluloses: Fundamentals and applications as new bio-based nanomaterials," *J. Wood Sci.* 59, 449-459. DOI: 10.1007/s10086-013-1365-z

Ítalo, P., Márcio, H., Ferreira, S., and Reinaldo, F. (2017). "Estimation of cellulose crystallinity of sugarcane biomass using near infrared spectroscopy and multivariate analysis methods," *Carbohyd. Polym.* 158, 20-28. DOI: 10.1016/j.carbpol.2016.12.005

Jiang, F., and Hsieh, Y. (2013). "Chemically and mechanically isolated nanocellulose and their self-assembled structures," *Carbohyd. Polym.* 95, 32-40. DOI: 10.1016/j.carbpol.2013.02.022

Jorfi, M., and Foster, E. (2015). "Recent advances in nanocellulose for biomedical applications," *J. Appl. Polym. Sci.* 132, 41719-41737. DOI: 10.1002/app.41719

Jung, Y., Chang, T., Zhang, H., Yao, C., Zheng, Q., Yang, V., Mi, H., Kim, M., Cho, S., Park, D., Jiang, H., Lee, J., Qiu, Y., Zhou, W., Cai, Z., Gong, S., and Ma, Z. (2015). "High-performance green flexible electronics based on biodegradable cellulose nanofibril paper," *Nat. Commun.* 6, 7170-7180. DOI: 10.1038/ncomms8170

Kargarzadeh, H., Ahmad, I., Abdullah, I., Dufresne, A., Zainudin, S., and Sheltami, R. (2012). "Effects of hydrolysis conditions on the morphology, crystallinity, and thermal stability of cellulose nanocrystals extracted from kenaf bast fibers," *Cellulose* 19, 855-866. DOI: 10.1007/s10570-012-9684-6

Kontturi, E., Laaksonen, P., Linder, M., Nonappa, Gröschel, A., and Rojas, O. (2018). "Advanced materials through assembly of nanocelluloses," *Adv. Mater.* 30, 1703779-1703418. DOI: 10.1002/adma.201703779

Liu, Y., Wang, H., Yu, G., Yu, Q., Li, B., and Mu, X. (2014). "A novel approach for the preparation of nanocrystalline cellulose by using phosphotungstic acid," *Carbohyd. Polym.* 110, 415-422. DOI: 10.1016/j.carbpol.2014.04.040

Lu, Y., Sathasivam, S., Song, J., Crick, C., Carmalt, C., and Parkin, I. (2015). "Robust self-cleaning surfaces that function when exposed to either air or oil," *Science* 347, 1132-1135. DOI: 10.1126/science.aaa0946

Mithilesh, Y., and Fang-Chyou, C. (2019). "Cellulose nanocrystals reinforced κ-carrageenan based UV resistant transparent bio-nanocomposite films for sustainable packaging applications," *Carbohyd. Polym.* 211, 181-194. DOI: 10.1016/j.carbpol.2019.01.114

Moon, R. J., Schueneman, G.T., and Simonsen, J. (2016). "Overview of cellulose nanomaterials, their capabilities and applications," *Jom.* 68, 2383-2394. DOI: 10.1007/s11837-016-2018-7

Narkpiban, K., Sakdaronnarong, C., Nimchua, T., Pinmanee, P., Thongkred, P., and Poonsawat, T. (2019). "The effect of mechano-enzymatic treatment on the characteristics of cellulose nanofiber obtained from kenaf (*Hibiscus cannabinus L.*) bark," *BioRes.* 14(1), 99-119. DOI: 10.15376/biores.14.1.99-119

Niu, F., Li, M., Huang, Q., Zhang, X., Pan, W., Yang, J., and Li, J. (2017). "The characteristic and dispersion stability of nanocellulose produced by mixed acid hydrolysis and ultrasonic assistance," *Carbohyd. Polym.* 165, 1970-204. DOI: 10.1016/j.carbpol.2017.02.048

Saito, T., Yanagisawa, M., and Isogai, A. (2005). "TEMPO-mediated oxidation of native cellulose: SEC–MALLS analysis of water-soluble and insoluble fractions in the oxidized products," *Cellulose* 12, 305-315. DOI: 10.1007/s10570-004-5835-8

Segal, L., Creely, J., Martin, A., and Conrad, C. (1959). "An empirical method for estimating the degree of crystallinity of native cellulose using the X-Ray diffractometer," *Text. Res. J.* 29, 786-794. DOI: 10.1177/004051755902901003

Sun, X., Wu, Q., Ren, S., and Lei, T. (2015). "Comparison of highly transparent all-cellulose nanopaper prepared using sulfuric acid and tempo-mediated oxidation methods," *Cellulose* 22, 1123-1133. DOI: 10.1007/s10570-015-0574-6

Sun, X., Wu, Q., Zhang, X., Ren, S., Lei, T., Li, W., Xu, G., and Zhang, Q. (2017). "Nanocellulose films with combined cellulose nanofibers and nanocrystals: tailored thermal, optical, and mechanical properties," *Cellulose* 25, 1103-1115. DOI: 10.1007/s10570-017-1627-9

TAPPI T 507 cm-99 (1999). "Grease resistance of flexible packaging materials," TAPPI Press, Atlanta, GA.

TAPPI T 494 om-13 (2013). "Tensile properties of paper and paperboard (using constant rate of elongation apparatus)," TAPPI Press, Atlanta, GA.

TAPPI T 460 om-11 (2011). "Air resistance of paper (Gurley method)," TAPPI Press, Atlanta, GA.

Tyagi, P., Lucia, L. A., Hubbe, M. A., and Pal, L. (2019). "Nanocellulose-based multilayer barrier coatings for gas, oil, and grease resistance," *Carbohyd. Polym.* 206, 281-288. DOI: 10.1016/j.carbpol.2018.10.114

Wang, Q., Zhao, X., and Zhu, J. (2014). "Kinetics of strong acid hydrolysis of a bleached kraft pulp for producing cellulose nanocrystals (CNCs)," *Ind. Eng. Chem. Res.* 53,

11007-11014. DOI: 10.1021/ie501672m

Wang, Q., Zhu, J., Reiner, R., Verrill, S., Baxxa, U., and McNeil, S. (2012). "Approaching zero cellulose loss in cellulose nanocrystal (CNC) production: recovery and characterization of cellulosic solid residues (CSR) and CNC," *Cellulose* 19, 2033-2047. DOI: 10.1007/s10570-012-9765-6

Wang, R., Chen, L., Zhu, J., and Yang, R. (2017). "Tailored and integrated production of carboxylated cellulose nanocrystals (CNC) with nanofibrils (CNF) through maleic acid hydrolysis," *Chem. Nano Mat.* 3, 328-335. DOI: 10.1002/cnma.201700015

Wang, W., Mozuch, M., Sabo, R., Kersten, P., Zhu, J., and Jin, Y. (2016). "Endoglucanase post-milling treatment for producing cellulose nanofibers from bleached eucalyptus fibers by a supermasscolloider," *Cellulose* 23, 1859-1870. DOI: 10.1007/s10570-016-0946-6

Wu, S., Buthe, A., Jia, H., Zhang, M., Ishii, M., and Wang, P. (2013). "Enzyme-enabled responsive surfaces for anti-contamination materials," *Biotech. Bioeng.* 110, 1805-1810. DOI: 10.1002/bit.24847

Xu, W., Grénman, H., Liu, J., Kronlund, D., Li, B., Backman, P., Peltonen, J., Willfor, S., Sundberg, A., and Xu, C. (2017). "Mild oxalic-acid-catalyzed hydrolysis as a novel approach to prepare cellulose nanocrystals," *Chem. Nano Mat.* 3, 109-119. DOI: 10.1002/cnma.201600347

Article submitted: October 2, 2019; Peer review completed: December 14, 2019; Revised version received and accepted: December 17, 2019; Published: December 18, 2019.
DOI: 10.15376/biores.15.1.1014-1025